Quantum Sieving in Single-Walled Carbon Nanotubes: Effect of Interaction Potential and Rotational−Translational Coupling

Giovanni Garberoglio,[†,‡] Michael M. DeKlavon,[‡] and J. Karl Johnson*[,†,‡]

National Energy Technology Laboratory, Pittsburgh, Pennsylvania 15236, and Department of Chemical Engineering, University of Pittsburgh, Pittsburgh, Pennsylvania 15261

Received: August 11, 2005; In Final Form: November 11, 2005

The selective adsorption of heavy isotopes in narrow nanotubes, known as quantum sieving, is studied using a simple approximate theory for several different potential models. We address the reasons for wide disagreement among previously published results for quantum sieving. We analyze the sensitivity of quantum sieving to perturbations in the potential parameters used in the calculations. The selectivities are very sensitive to changes in the atomic diameter parameter and less sensitive to changes in the potential well depth. We present an approximate method for accounting for rotational−translational coupling that is computationally efficient and accurate for the narrowest nanotubes. For wide nanotubes, the estimation of rotational−translational coupling becomes inaccurate because of neglect of the effect of rotational states on the translational degrees of freedom.

I. Introduction

The adsorption of gases on single-walled carbon nanotubes (SWNTs) has been extensively studied, both experimentally and theoretically.[1−18] The interest in SWNTs as sorbents is due in part to the unusual one-dimensional nature of the internal (endohedral), groove, and interstitial sites found within bundles of SWNTs.

One of the most interesting and dramatic predictions made for adsorption of gases in SWNTs is that narrow SWNTs can be used to separate light isotopes with remarkably high selectivities.[19−25] The separation of isotopes in nanopores has been called quantum sieving because the separation is caused by differences in the quantum energy levels of the isotopes being separated. Quantum sieving of hydrogen isotopes in SWNTs could potentially be an energy-efficient and cost-effective separation technology. Direct experimental confirmation of quantum sieving in SWNTs is still lacking. However, the work of Wilson et al., showing a difference in the isosteric heats of D_2 and H_2 adsorbed on the external surface of SWNT bundles,[17] and the work of Tanaka et al., showing differences in D_2 and H_2 isotherms on opened single-wall carbon nanohorns,[26] provide indirect evidence for quantum sieving in nanotube systems.

The isotope effect in adsorption has been known for many years.[27,28] However, Beenaker et al.[29] were the first to propose that quantum sieving would be observed in narrow channels when the diameter of the pore is close to the value of the hard core separation of the adsorbates. Their predictions were based on a very simple model involving only hard spheres in a cylindrical well. Challa et al.[19−21] calculated the selectivity of hydrogen isotope mixtures in SWNTs. They used a spherically symmetric potential for hydrogen and a realistic description of the H_2−SWNT potential. They used a simple theory to compute the selectivity in the limit of zero pressure and tested their theory against rigorous path integral Monte Carlo simulations. They also predicted finite pressure selectivities and isotherms using path integral grand canonical Monte Carlo. Gordillo et al.[22] used the Stan−Cole potential[30] for the H_2−SWNT interactions in conjunction with diffusion Monte Carlo simulations to obtain zero-pressure selectivities for hydrogen isotopes in SWNTs. The Stan−Cole model assumes a spherically symmetric H_2 molecule. Hathorn et al.[23] were the first to investigate the effect of the hydrogen molecule's structure on the selectivity. They calculated the contribution to the selectivity due to the rotational degrees of freedom, under the assumption that the center of mass of the molecules is fixed at the bottom of the solid−fluid potential well. Their results indicate that hindered molecular rotations contribute substantially to the overall selectivity. Assuming uncoupled translational and rotational degrees of freedom, their findings imply that taking rotations into account would increase the total selectivity by a factor of the order of 100 over the translational selectivity in nanotubes with a radius close to that of the (3, 6) SWNT at 20 K. Trasca et al.[25] used a rigid rotor model for H_2 developed by Kostov et al.[31] and quantum mechanical simulations to obtain selectivities in the interstitial and groove sites of a (18, 0) nanotube bundle. They considered both translational confinement and rotational hindrance, finding selectivities for H_2/D_2 in SWNT interstices that are orders of magnitude larger than those predicted by Challa et al.[21] Lu et al.[24] used a semiempirical Tersoff−Brenner potential with an exact quantum mechanical formalism to solve the full quantum mechanical problem of a confined rigid rotor. They obtained the selectivities for various hydrogen isotopes in the zero-pressure limit for five different nanotubes, accounting for both translational and rotational quantum states. Their computed selectivities were orders of magnitude smaller than those predicted by Challa et al. for very narrow nanotubes.

A summary of some of the selectivities calculated by four different groups is presented in Table 1. It is evident that there is a lack of agreement between calculations performed by different groups. The predicted values of the selectivities differ by orders of magnitude in some cases. Two of the groups represented in Table 1 considered only translational selectivities,

* Corresponding author. E-mail: karlj@pitt.edu.
† National Energy Technology Laboratory.
‡ University of Pittsburgh.

10.1021/jp054511p CCC: $33.50
Published on Web 01/07/2006

TABLE 1: Comparison of Zero-Pressure Selectivities Computed from Various Groups

	group results			
system	Challa et al.[20,21]	Gordillo et al.[22]	Lu et al.[24]	Trasca et al.[25]
(3, 6) T_2/H_2	1.47×10^5		69.58	
(5, 5) T_2/H_2	417	22.8		
(10, 10) T_2/H_2	~9		20.52	
(10, 10) interstice D_2/H_2	~700			$\sim 10^{9a}$

[a] The interstice used by Trasca et al. was for a bundle of (18, 0) SWNTs, which have a diameter close to that of the (10, 10) SWNT.

namely, Challa et al.[20,21] and Gordillo et al.[22] The other two, Lu et al.[24] and Trasca et al.,[25] include both translational and rotational effects. It is not clear to what extent coupling between rotational and translational degrees of freedom affects the energy levels and, consequently, the zero-pressure selectivities.

The purposes of this paper are as follows: first, to identify reasons for the widely different selectivities computed by the various groups; second, to assess the sensitivity of quantum sieving to changes in the solid−fluid potentials used in the calculations; and third, to estimate the importance of rotational−translational coupling on quantum sieving. To answer these questions, we investigate in detail the zero-pressure selectivity, S_0, of a T_2-H_2 mixture in a (3, 6) SWNT at 20 K with various different potentials. We present an approximate method to evaluate the contribution of rotational−translational coupling on the selectivity in narrow tubes and apply it to the model potentials within the rigid rotor approximation. The results computed with our approximate method are compared with results obtained by Lu et al.[32] for a number of different nanotubes using an exact method in the zero-pressure limit.

II. Methods

The selectivity of species i relative to species j is defined as

$$S(i/j) = \frac{x_i/x_j}{y_i/y_j} \tag{1}$$

where x_i and y_i are the mole fractions in the adsorbed and bulk phases, respectively. In the limit of zero pressure, when one can neglect the adsorbate−adsorbate interactions, the selectivity depends only on the energy levels E_i^l of the adsorbed molecules and can be written as[21,23]

$$S_0(i/j) = \frac{Q_j^{\text{free}}}{Q_i^{\text{free}}}\frac{Q_i}{Q_j} = \frac{m_j}{m_i}\frac{Q_j^{\text{free-rot}}}{Q_i^{\text{free-rot}}}\left[\frac{\sum_l \exp(-E_i^l/(kT))}{\sum_l \exp(-E_j^l/(kT))}\right] \tag{2}$$

where Q_i^{free} is the molecular partition function of an ideal gas, $Q_i^{\text{free-rot}}$ is the free rotor partition function, and Q_i is the molecular partition function for the adsorbed species i.

The zero-pressure selectivity can be factored into the product of two contributions by assuming that the translational and rotational degrees of freedom are uncoupled,

$$S_0 = S_{\text{trans}} S_{\text{rot}} \tag{3}$$

where S_{trans} depends only on the translational and S_{rot} only on the rotational degrees of freedom. The assumption that the translational and rotational degrees of freedom are uncoupled is an excellent approximation for H_2 in the gas, liquid, and even low-pressure solid phases. We will show, however, that rotational−translational coupling is very important for hydrogen isotopes adsorbed in narrow SWNTs.

II.A. The Potential Models. We have chosen the standard 12−6 Lennard-Jones (LJ) potential to model carbon−hydrogen interactions in our calculations,

$$V_{\text{LJ}}(r) = 4\epsilon_{\text{HC}}\left[\left(\frac{\sigma_{\text{HC}}}{r}\right)^{12} - \left(\frac{\sigma_{\text{HC}}}{r}\right)^{6}\right] \tag{4}$$

where σ_{HC} is the LJ diameter parameter for H−C interactions and ϵ_{HC} is the well-depth. These parameters were obtained by applying the Lorentz−Berthelot combining rules to the pure component interaction parameters.

The sets of potential parameters used for our calculations are reported in Table 2. The first two potentials listed in Table 2 assume that the H_2 molecule can be modeled as a single LJ sphere with parameters taken from Buch.[33] The Buch LJ potential has been shown to reproduce the equation of state for pure fluid hydrogen over a wide range of temperatures and densities.[34] The remaining four potentials treat H_2 as a rigid diatomic with a bond length $l = 0.74$ Å.

The values of the LJ parameters in Table 2 for the spherical H_2 potential are for $C-H_2$ interactions, whereas for the atom explicit potentials σ_{HC} and ϵ_{HC} refer to atom−atom interactions.

As a general trend, we notice that the values of σ_{HC} are around 3.15 Å for the H_2-C models and about 3.0−3.1 Å for the atom−atom models, except for the Brenner−Lu potential,[24] for which $\sigma_{\text{HC}} = 2.531$ Å. The reason for the unusually small value of σ_{HC} in the Brenner−Lu potential is that Lu and co-workers mistakenly used an unrealistically small value of σ_{CC}. The potential actually used in ref 24 includes both a reactive bond-order potential for C−H interactions with the LJ term added in at longer distances to account for dispersion.[35] However, Lu et al. multiplied the LJ potential by a spurious factor of 2 in their calculations.[24,36]

We have generated effective spherical potentials for the diatomic potentials listed in Table 2 in order to compare our results with previous calculations[19−21] and to assess the magnitude of rotational quantum effects. The spherical potentials were generated by computing the minimum value of the potential for each value of r, the distance from the center of the nanotube. The full potential is described by the location of the center of mass and the orientation of the H_2 molecule. We chose r to lie along the x-axis and computed the potentials at $z = 0$ in the unit cell. The orientation of the molecule was optimized at each value of r, and the resulting potential was used in the calculations. This procedure gives the widest possible potential energy profile and consequently, as will be apparent in the following, the minimum value of S_0.

Due to the chiral nature of the (3, 6) tube, the calculations along the direction $-x$ as well as along an orthogonal direction y yielded different values for the solid−fluid potential energy. As an example, the potential energy calculated using the Frankland−Brenner (FB) parameters[35] near the wall is lower along the $-x$ axis than along the $+x$ axis, and the opposite is true for the y axis. This energy difference at either side of the tube is due to the hydrogen molecule approaching either the center of a hexagonal face or a carbon atom. The values we obtain are $V(x = 0.643) = 3590$ K and $V(x = -0.643) = 3330$ K, which is a difference of about 7%, whereas on the orthogonal direction $V(y = -0.643$ Å) has only a 0.3% difference from $V(y = 0.643)$.

The effect of the asymmetry of the potential is of course less pronounced for points closer to the tube axis, and so, given the

TABLE 2: Lennard-Jones Parameters for Different Potential Models[a] Considered in This Work

parameter set	σ_{HC} (Å)	ϵ_{HC} (K)	σ_{CC} (Å)	ϵ_{CC} (K)	σ_{HH} (Å)	ϵ_{HH} (K)
Brenner[35]−Buch[38] (s)	3.155	41.845	3.35	51.2	2.96	34.2
Steele[39]−Buch[38] (s)	3.180	30.945	3.40	28.0	2.96	34.2
Brenner−Lu[24] (r)	2.545	20.984	2.28	51.2	2.81	8.6
FB[35] (r)	3.080	27.713	3.35	51.2	2.81	15.0
AIREBO[40] (r)	3.020	23.952	3.40	32.957	2.64	17.407
Steele−Murad[41] (r)	3.105	15.518	3.40	28.0	2.81	8.6

[a] The s denotes a spherical model and r denotes a rigid diatomic model for H_2. The parameters for diatomic models refer to the hydrogen atom sites.

small difference in the potential energy along different directions, we have assumed the potential to be radially symmetric.

In the case of two-site models we evaluate the potential on one site by taking an average, in cylindrical coordinates, along the angle Θ and along one unit cell in the z direction. The resulting potential is then a function of the orientation (θ, ϕ) of the diatomic and the distance r of the molecule's center of mass from the nanotube axis.

II.B. Calculation of the Selectivity from the Translational Degrees of Freedom. The potential along the x axis was fitted with an eighth order polynomial, as in previous work.[10] We found the energy levels by taking the smoothed potential and calculating the Hamiltonian matrix in the basis of a 2D harmonic oscillator. The effective frequency of the harmonic oscillator was set by two methods according to whether the potential was flat or parabolic in nature. For the flatter, nonharmonic potentials, such as potentials generated by Brenner−Lu values, the effective frequency was estimated so that the size of l of the ground state is comparable with the size of the potential "plateau", using the formula

$$\omega = \frac{\hbar}{ml^2} \tag{5}$$

For the potentials that were more harmonic in nature, the effective frequency was taken as the square root of the second derivative of the potential function divided by the mass of the molecule.

We found that a larger matrix was needed to converge the energy levels properly for flatter potentials. It was found that a 900 by 900 matrix was large enough to converge the energy levels, and this was used in all the calculations. A few test runs using a 1600 by 1600 matrix yielded differences in the eigenvalues of less than 1 K.

II.C. The Rotational Degrees of Freedom. Hathorn et al. showed that quantum sieving can result purely from the rotational degrees of freedom in narrow nanotubes.[23] It is known that translational and rotational degrees of freedom are coupled for hydrogen confined in narrow tubes,[37] but it is not yet known how this coupling influences the selectivity. In this section we first consider the uncoupled case and then derive an approximate expression that allows for coupling between the translational and rotational states.

If we suppose the hydrogen molecule is fixed with the center of mass at a distance r from the tube axis and assume a smoothed potential as described in section II.A, the rotational Hamiltonian is

$$\hat{H}_{rot} = \frac{\hat{L}^2}{2I} + \hat{V}(r; \theta, \phi) \tag{6}$$

where $\hat{L}$ is the rotational momentum operator. In this case, the selectivity depends only on the rotational degrees of freedom and the value of the parameter r. The rotational selectivity can be calculated using eq 2 as[23]

$$S_{rot}(r) = \frac{Q_{H_2}^{free-rot}}{Q_{T_2}^{free-rot}} \frac{Q_{T_2}^{fixed-rot}(r)}{Q_{H_2}^{fixed-rot}(r)} \tag{7}$$

where $Q^{free-rot}$ is the free rotor partition function and $Q^{fixed-rot}(r)$ is the rotational partition function for a confined diatomic fixed at a distance r from the nanotube axis. We have chosen to simulate para-H_2 and para-T_2, so that the sum in the partition function is restricted to even angular momentum states only.

The spectrum of the confined rotor can be obtained directly by diagonalizing the Hamiltonian in eq 6, using the even angular momentum states of a free rotor as a basis set. These states are the spherical harmonics $\langle \theta, \phi | lm \rangle = Y_m^l(\theta\phi)$ with even angular momentum l. Since a cylindrically symmetric potential is invariant under reflection on any plane containing the symmetry axis, one has $V(r; \theta, \phi) = V(r; \theta, -\phi)$, and as a consequence, the matrix elements $\langle l'm' | \hat{V}(r; \theta, \phi) | lm \rangle$ are real. Moreover, due to the diatomic nature of our molecule and the assumption of a cylindrically symmetric potential, we have $V(r; \theta, \phi) = V(r; \theta, (\pi - \phi))$, which implies $\langle l'm' | \hat{V}(r; \theta, \phi) | lm \rangle = 0$ if $m + m'$ is odd.[37] We note that good convergence is obtained in our calculations by taking into account angular momenta up to $l = 12$ (corresponding to a 91 by 91 Hamiltonian matrix) regardless of the value of the radial coordinate r.

A first estimate of the effect of the rotational degrees of freedom to the overall selectivity can be made assuming complete decoupling of the translational and rotational contributions, as in eq 3. The rotational contribution can be calculated from eq 7 with the eigenvalues of the rotational Hamiltonian, eq 6, at the minimum of the potential well.[23]

The full Hamiltonian for a hydrogen molecule confined in an external potential $V(r; \theta, \phi)$ is

$$\hat{H} = \hat{K}_{CM} + \hat{K}_{rot} + \hat{V}(r; \theta, \phi) \tag{8}$$

where $\hat{K}_{CM}$ is the center of mass kinetic energy and $\hat{K}_{rot}$ is the rotational kinetic energy. It is clear that the translational and rotational degrees of freedom are coupled by the potential V, and this will have an effect on the eigenvalues and hence on the selectivity of the system.

In principle, the selectivity must be computed by solving eq 8 for the full spectrum of energy levels and inserting these into eq 2.[24] To investigate the effect of the rotational−translational coupling on the selectivity, we develop an approximation to the partition function corresponding to the Hamiltonian of eq 8, which is given by

$$Q = \sum_{t,R} \langle t, R | \exp(-\beta \hat{H}) | t, R \rangle \tag{9}$$

where $|t, R\rangle = |t\rangle|R\rangle$ is a basis set obtained by the product of

two complete basis sets $|t\rangle$ and $|R\rangle$ for the translational and rotational degrees of freedom, respectively.

In a steep potential, one expects from a semiclassical point of view that there is a very high probability that a molecule will be aligned with the nanotube axis, since the energy for a rotation of an angle θ satisfies $|V(r; \theta, \phi) - V(r; 0, 0)| \gg k_B T$ for a small value of θ.[24] The potential energy for this case can be written as

$$\hat{V}(r; \theta, \phi) = \hat{V}_{||}(r) + \Delta\hat{V}(r; \theta, \phi) \tag{10}$$

where we have denoted by $\hat{V}_{||}(r) = \hat{V}(r; \theta = 0, \phi = 0)$ the potential energy for a molecule whose axis is parallel to the nanotube axis. For H_2 $V_{||}(r)$ is actually twice the potential energy acting on one hydrogen atom at a distance r from the nanotube axis.

A further simplification of eq 9 can be obtained if we assume that

$$\exp(-\beta\hat{H}) \simeq \exp[-\beta(\hat{K}_{CM} + \hat{V}_{||})] \exp[-\beta(\hat{K}_{rot} + \Delta\hat{V})] \tag{11}$$

In this case, the partition function can be written as

$$Q \simeq \sum_{t,R} \langle t, R| \exp[-\beta(\hat{K}_{CM} + \hat{V}_{||})] \exp[-\beta(\hat{K}_{rot} + \Delta\hat{V})] |t, R\rangle \tag{12}$$

$$= \sum_{t,R} \exp(-\beta E_t) \langle t, R| \exp[-\beta(\hat{K}_{rot} + \Delta\hat{V})] |t, R\rangle \tag{13}$$

$$= \sum_{t,R} \int dx\, dy\, dx'\, dy' \exp(-\beta E_t) \langle t|x, y\rangle \times \langle x, y; R| \exp[-\beta(\hat{K}_{rot} + \Delta\hat{V})] |x', y'; R\rangle \langle x', y'|t\rangle \tag{14}$$

$$= \sum_{t,R} \int dx\, dy \exp(-\beta E_t)\, |\psi_t(x, y)|^2 \times \langle R| \exp[-\beta(\hat{K}_{rot} + \Delta\hat{V})] |R\rangle \tag{15}$$

$$= \sum_{t,R} \int dx\, dy \exp(-\beta E_t)\, |\psi_t(x, y)|^2 \exp[-\beta E_R \sqrt{x^2 + y^2}] \tag{16}$$

$$= Q^{trans} \int 2\pi r\, dr\, \rho(r) \sum_R \exp[-\beta E_R(r)] \tag{17}$$

$$= Q^{trans} \int 2\pi r\, dr\, \rho(r) Q^{rot}(r) \tag{18}$$

where we have used as a complete set for the translational degrees of freedom the eigenstates of the translational Hamiltonian $[\hat{K}_{CM} + \hat{V}_{||}(r)]|t\rangle = E_t|t\rangle$, whose spatial wave function is $\psi_t(x, y) = \langle x, y|t\rangle$. We denote by $\rho(r)$ the radial thermal density, defined as

$$\rho(r) = \int \frac{d\Theta}{2\pi} \frac{\sum_t \exp(-\beta E_t) |\psi_t(r \cos\Theta, r \sin\Theta)|^2}{\sum_t \exp(-\beta E_t)} \tag{19}$$

and normalized so that $\int \rho(r)\, 2\pi r\, dr = 1$. We have introduced the translational partition function

$$Q^{trans} = \sum_t \exp(-\beta E_t) \tag{20}$$

obtained from the energy levels E_t of a molecule aligned with the nanotube axis. The position dependent rotational partition function is defined as

$$Q^{rot}(r) = \sum_R \exp[-\beta E_R(r)] \tag{21}$$

and is obtained by summing the Boltzmann factors of the energy spectrum of the rotational Hamiltonian, $\hat{H}_{rot} = \hat{K}_{rot} + \hat{V}(r; \theta, \phi) - V_{||}(r)$, with r treated as a parameter.

We can now write the selectivity by substituting eq 18 into eq 2, obtaining

$$S_0(T_2/H_2) = \left(\frac{m_{H_2}}{m_{T_2}} \frac{Q^{trans}_{T_2}}{Q^{trans}_{H_2}}\right) \left(\frac{Q^{free-rot}_{H_2}}{Q^{free-rot}_{T_2}} \frac{\int r\, dr\, \rho_{T_2}(r) Q^{rot}_{T_2}(r)}{\int r\, dr\, \rho_{H_2}(r) Q^{rot}_{H_2}(r)}\right) \tag{22}$$

Equation 22 factorizes into the product of the translational selectivity

$$S_{trans} = \frac{m_{H_2}}{m_{T_2}} \frac{Q^{trans}_{T_2}}{Q^{trans}_{H_2}} \tag{23}$$

and rotational selectivity, including (approximately) the rotational−translational coupling,

$$S_{rot-trans} = \frac{Q^{free}_{H_2}}{Q^{free}_{T_2}} \frac{\int 2\pi r\, dr\, \rho_{T_2}(r) Q^{rot}_{T_2}(r)}{\int 2\pi r\, dr\, \rho_{H_2}(r) Q^{rot}_{H_2}(r)} \tag{24}$$

If there is no coupling between rotational and translational degrees of freedom then $S_{rot-trans} = S_{rot}$. Likewise, in the free-rotor limit, $S_{rot-trans} = 1$, and so the selectivity is determined only by the quantization of the translational degrees of freedom. This will be the case for very broad potentials, such as the Brenner−Lu potential for the (3, 6) nanotube (see Figure 1).

In the limit where all the density is concentrated on the tube axis, that is, $\rho(r) = \delta(r)/(2\pi r)$, we recover the approximate result of eq 3, which assumes decoupling of the translational and rotational degrees of freedom. In practice, quantum effects in narrow potentials ensure that the density is never located only on the tube axis, so the rotational and translational degrees of freedom are always coupled for highly confined systems.

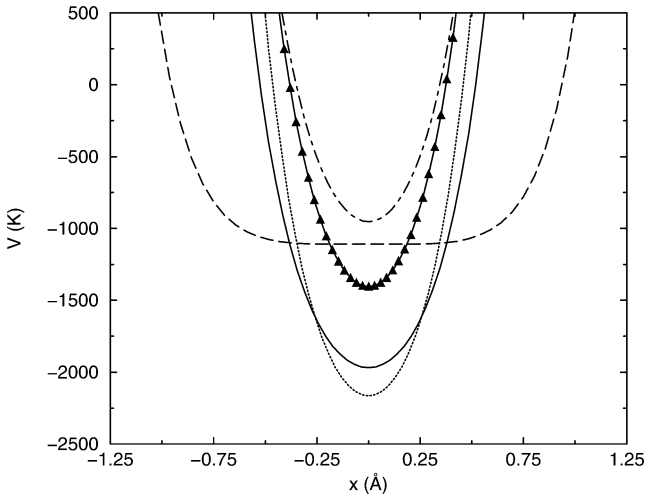

Figure 1. Potential energy curves for H_2 inside a (3, 6) SWNT from five potential parameter sets identified in Table 2: Brenner−Lu[24] (dashed line), Frankland−Brenner[35] (dotted line), Brenner−Buch[35,38] (triangles), AIREBO[40] (solid line), and Steele−Buch[38,39] (dot−dashed line).

TABLE 3: $S_0(T_2/H_2)$ Computed for the (3, 6) SWNT at 20 K Using Effective Spherical Potentials Generated As Described in the Text

parameter set	unaltered parameters	$\sigma_{CC} + 10\%$	$\sigma_{CC} - 10\%$	$\epsilon_{CC} \times 2$	$\epsilon_{CC}/2$
Brenner−Buch	6.05×10^5	1.74×10^8	7.68×10^3	7.51×10^6	7.20×10^4
Steele−Buch	1.80×10^5	2.71×10^7	3.46×10^3	1.80×10^6	2.63×10^4
Brenner−Lu	10.03	34.19	4.95	16.93	6.79
FB	3.72×10^5	1.29×10^8	4.45×10^3	4.24×10^6	4.84×10^4
AIREBO	2.98×10^4	4.44×10^6	724	2.16×10^5	5.79×10^3
Steele−Murad	2.63×10^4	2.55×10^6	792	1.83×10^5	5.13×10^3

D. Discussion of the Approximations. The derivation of eq 22 depends on the validity of two assumptions: (1) a molecule being almost aligned with the nanotube axis and (2) the neglect of a commutator in eq 11. We expect the first condition to be very well fulfilled in narrow nanotubes. We assume that in this case the ground state of the system does not present spherical symmetry as the $l = 0$, $m = 0$ ground state of the free rotor.

We note that in eq 22 the density is given by the solution of the "translational" Hamiltonian (see eq 20), assuming a molecule perfectly aligned with the SWNT axis. Because of the neglect of the commutation relations in eq 11, we take into account the effect of the translational degrees of freedom on the rotational dynamics, but we do not take into account the effect of the rotational degrees of freedom on the center of mass dynamics.

Consider, for example, a molecule in a narrow potential (i.e., $|V(r; \theta, \phi) - V(r; 0, 0)| \gg k_B T$ for small values of θ) whose center of mass is at a distance r from the nanotube axis. Since the molecule is almost perfectly aligned with the nanotube axis, the quantum fluctuations of the molecular directions have only a negligible influence on the "force" acting on the center of mass degrees of freedom. The translational wave function is very well approximated by the wave function of a molecule perfectly aligned with the tube axis.

On the other hand, if the potential energy profile is wide enough (i.e., $|V(r; \theta, \phi) - V(r; 0, 0)| \sim k_B T$), the effective potential energy on the center of mass will depend critically on the orientational degrees of freedom. In this case, our approximation is likely to be inaccurate because it does not include the effect of the rotational state on the center of mass wave function. It follows that we expect our approximation to be less and less reliable for tubes with a potential energy profile "wider" than the (3, 6).

III. Results

The effective solid−fluid spherical potentials calculated according to the procedure described in section II.B are plotted in Figure 1. Note that the Brenner−Lu potential exhibits a very flat region up to a distance of about 0.6 Å from the nanotube axis. This potential is qualitatively different from the others, which all display a well-defined minimum and a steep increase going toward the tube surface. The potential energy profile for the Brenner−Lu potential does not coincide with the one reported by Lu and co-workers,[24] who have introduced an extra factor of 2. [36] In addition, their potential exhibits several minima in the potential as r increases. These minima are the result of the reactive part of the potential becoming important as the H_2 molecule approaches a carbon atom. We have used only the LJ part of the potential, so that reactions are not allowed.

Aside from the Brenner−Lu potential, all the other potentials are qualitatively similar in shape. The widths of the potentials, defined, for example, at $V(r) = 0$, range from about $r = 0.7$ to $r = 1.0$ Å. The well depths show a wider variation, ranging from −900 K for the Steele−Buch potential to −2100 K for the FB parameters.

III.A. Selectivity in the Spherical Approximation. We have computed zero-pressure selectivities for spherical H_2 (assuming that the H_2 molecule behaves as a free rotor) for the potentials listed in Table 2. The results from these calculations are reported in Table 3. Our purpose in performing these calculations was to assess the sensitivity of S_0 to the specific potential used in the calculations. As expected, the Brenner−Lu potential results in the lowest selectivity of all the potentials examined, giving $S_0 = 10.03$, whereas all the other potentials exhibit selectivities in the range 10^4-10^5. The very small value of S_0 obtained from the Brenner−Lu potential is a direct result of using an unphysical value of σ_{CC}, thereby giving a very flat potential.

As a general trend, we note that the selectivity increases with the steepness of the potential. This is expected since, from eq 2, it is the difference in level separations between the two isotopes rather than the magnitude of the potential energy that determines the zero-pressure selectivity. Taking the harmonic oscillator as an example, the spacing would be given by $\Delta E = \hbar(\omega_{H_2} - \omega_{T_2})/2 = \hbar((k/m_{H_2})^{1/2} - (k/m_{T_2})^{1/2})/2$, which is a function of the steepness of the potential (the spring constant k, i.e., the second derivative of the potential) and not of the absolute magnitude of the levels. This is apparent by comparing the results for the AIREBO (adaptive intermolecular reactive empirical bond-order) potential[40] to the FB potential. Both potentials have almost the same potential minimum, around −2000 K (see Figure 1), but the AIREBO is less steep, resulting in a selectivity of 2.98×10^4 whereas the steeper FB potential gives a result of 3.72×10^5, an order of magnitude higher.

We see from the data in Table 3 that six of the potentials give S_0 values that are in qualitative agreement, indicating that the T_2/H_2 selectivity is predicted to be extraordinarily large in the (3, 6) SWNT, independent of the details of the potential model used, as long as the potential parameters are physically reasonable. Only the Brenner−Lu potential gives results that do not qualitatively agree with the other potentials. On the other hand, the exact value of S_0 varies by over an order of magnitude, depending on which potential model is chosen.

We have investigated the sensitivity of the selectivity to specific changes in the LJ diameter, σ, and the potential well depth, ϵ. We have changed the LJ diameter of the carbon potential by ±10%. The carbon well depth has been changed by a much larger amount, multiplying or dividing by a factor of 2. These changes in σ_{CC} and ϵ_{CC} change the solid−fluid potential parameters through the Lorentz−Berthelot combining rules.

The effect of changing the LJ diameter on the potential energy curves is shown in Figure 2. The net effect of a larger σ_{CC} is to increase the steepness of the potential, with an opposite trend observed for smaller values of σ_{CC}. The result of these changes on the selectivity is rather dramatic for most potentials, as is shown in Table 3. Increasing σ_{CC} by 10% gives selectivities that are typically at least 2 orders of magnitude larger than the unmodified potentials. Likewise, decreasing the LJ diameter by 10% decreases the selectivity by about 2 orders of magnitude.

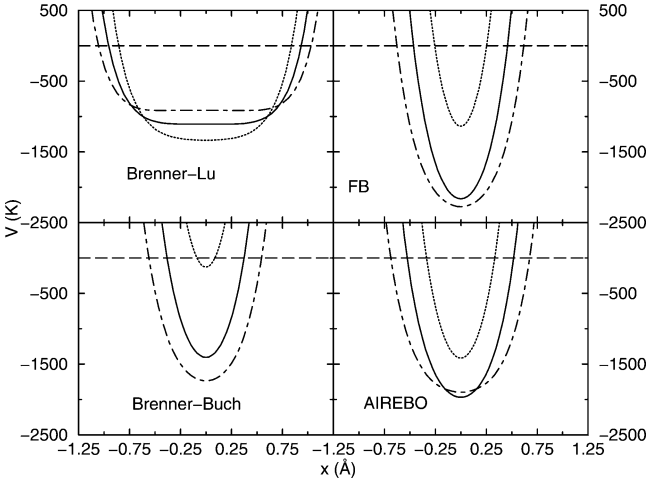

Figure 2. The effect of σ_{CC} on the potentials with σ_{CC} unaltered (solid line), σ_{CC} increased by 10% (dotted line), and σ_{CC} decreased by 10% (dot−dashed line).

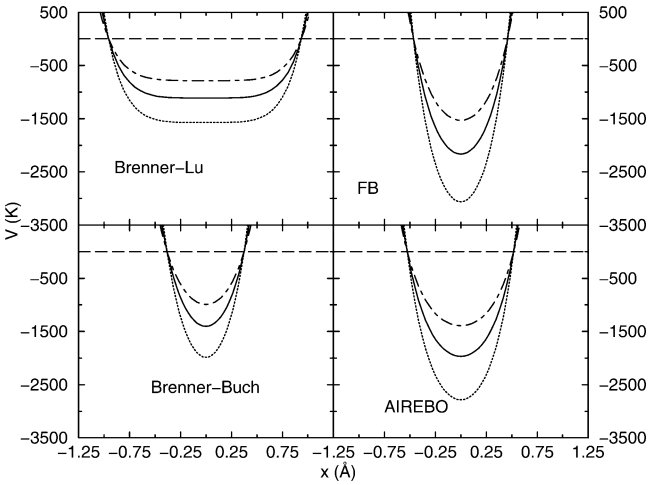

Figure 3. The effect of ϵ_{CC} on the potentials with ϵ_{CC} unaltered (solid line), ϵ_{CC} increased by 100% (dotted line), and ϵ_{CC} decreased by 50% (dot−dashed line).

The effect of scaling the potential by multiplying or dividing ϵ_{CC} by a factor of 2 always has a less dramatic effect than changing σ_{CC} by ±10%. Increasing the C−C well depth by a factor of 2 (which increases ϵ_{HC} by a factor of $2^{1/2}$) leads, in general, to an increase in S_0 of about 1 order of magnitude. Similarly, decreasing ϵ_{CC} by a factor of 2 gives roughly a decrease in the selectivity of 1 order of magnitude. Changes in the Brenner−Lu potential to ϵ_{CC} or σ_{CC} give relatively small changes in the selectivity compared with the other potentials.

We can observe that the steepness of the potential has a greater influence on the selectivity than the well depth by comparing the Brenner−Buch potential with $2\epsilon_{CC}$ and the unaltered AIREBO potential. The absolute value of the minima is comparable for these potentials (see Figure 3), whereas the former is steeper than the latter, resulting in a selectivity over 200 times larger for the Brenner−Buch $2\epsilon_{CC}$ potential. We also note that the unaltered Brenner−Buch potential has a minimum comparable to the AIREBO potential with $\epsilon_{CC}/2$ (see Figure 3), but the selectivities differ by 2 orders of magnitude.

III.B. The Rotational Degrees of Freedom. We report our findings for the influence of the rotational degrees of freedom on the selectivity in Tables 4 and 5. The translational selectivities were obtained by constraining a molecule to always be aligned with the nanotube axis (eq 23). These values, reported in Table 4, are in very good agreement with the results obtained with the effective spherical model (see Table 3), indicating that for a given distance from the nanotube axis, the configuration of minimum potential energy is the one with the molecule parallel to the nanotube axis. This is not the case for the Brenner−Lu potential, which is wide enough so that the minimum in the potential corresponds to an H_2 orientation almost perpendicular to the nanotube axis when the molecule is near the center of the tube.

TABLE 4: Contributions to the Selectivity for T_2/H_2 in the (3, 6) SWNT at 20 K for the Rigid Diatomic Models

parameter set	S_{rot} eq 7	$S_{rot-trans}$ eq 24	S_{trans} eq 23	S_0 $S_{trans}\cdot S_{rot-trans}$
Brenner−Lu	1.0	1.3	8.1	10.3
FB	2.1×10^4	4.5×10^4	3.3×10^5	1.51×10^{10}
AIREBO	1.03×10^3	2.3×10^3	3.1×10^4	7.2×10^7
Steele−Murad	750	1.65×10^3	2.4×10^4	4.06×10^7

The approximate effect of rotational−translational coupling on the overall selectivity in the (3, 6) tube is shown in Table 4. The results from the simple (uncoupled) model of eq 7 can be compared with the values obtained using the approximate treatment of the rotational−translational coupling given in eq 24. We note that our results for the effect of the rotational degrees of freedom for all realistic potentials, even in the framework of the simplest uncoupled approximation, eq 7, indicate that rotational quantization is very important in determining the selectivity of narrow nanotubes. The selectivity is enhanced by a factor between 750 and 21 000, depending on the steepness of the confining potential. These values are higher than the factor of ∼300 predicted by Hathorn and co-workers[23] for a tube with a diameter of the (3, 6) SWNT.

We have calculated the ground-state rotational kinetic energy for a molecule having its center of mass fixed along the (3, 6) axis for the potentials reported in Table 4. We obtain for H_2 a series of values in the range 340−454 K and for T_2 a series of values in the range 109−198 K, except for the case of the Brenner−Lu potential, where H_2 and T_2 have rotational kinetic energies of 0.02 and 0.18 K, respectively. The large rotational ground-state energy is a direct manifestation of what Lu and co-workers refer to as "extreme two-dimensional confinement".[32] The rotational ground state for extreme confinement includes contributions from the $l > 0$ spherical harmonics, meaning that the ground state is not spherically symmetric, but has a directional preference. This directional preference is quantified in Figure 4 for H_2 in a (3, 6) SWNT with the molecular center of mass located on the nanotube axis. The probability that a molecule has a given alignment with respect to the nanotube is plotted as function of the cosine of the angle in Figure 4 for the FB and the Brenner−Lu potentials. The probability is normalized such that

$$\int_{-1}^{1} P(\theta)\, \mathrm{d}\cos\theta = 1 \qquad (25)$$

The probability is at a maximum for $\theta = 0, \pi$ for the FB potential and virtually flat (i.e., spherically symmetric) for the Brenner−Lu potential. Therefore, our *ansatz* that $\theta \sim 0$ for very narrow nanotubes used in the derivation of eq 24 is justified a posteriori by the observation of large nonzero rotational kinetic-energy ground states. We note that $P(\theta)$ for the FB potential in Figure 4 is analogous to that in Figure 5 in ref 32 for the ground state. The main difference is that their probability is averaged over all r and our plot is only for $r = 0$.

The net effect of the rotational−translational coupling is to enhance the value given from the simple uncoupled model by a factor greater than 2, except in the case of the Brenner−Lu

TABLE 5: Contributions to the Selectivity as a Function of the Potential Parameters for T_2/H_2 in the (3, 6) SWNT at 20 K

	unaltered		$\sigma_{CC} + 10\%$		$\sigma_{CC} - 10\%$		$\epsilon_{CC} \times 2$		$\epsilon_{CC}/2$	
parameter set	S_{trans}	$S_{rot-trans}$	S_{trans}	$S_{rot-trans}$	S_{trans}	$S_{rot-trans}$	S_{trans}	$S_{rot-trans}$	S_{trans}	$S_{rot-trans}$
Brenner−Lu	8.1	1.3	25.8	1.6	3.95	1.04	11	1.31	6.2	1.2
FB	3.3×10^5	4.5×10^4	1.1×10^8	2.5×10^7	4.03×10^3	140	3.7×10^6	6.9×10^5	4.4×10^4	3.6×10^3
AIREBO	3.1×10^4	2.3×10^3	4.8×10^6	8.9×10^5	712	15.5	2.2×10^5	2.7×10^4	6.0×10^3	247
Steele−Murad	2.4×10^4	1.65×10^3	2.35×10^6	4.1×10^5	740	16	1.6×10^5	1.89×10^4	4.7×10^3	180

potential, for which the uncoupled approximation is relatively good. This can be understood from the fact that this potential shows a very flat region near the tube axis (see Figure 1), where most of the density is located. Because of the flatness of the potential, the rotation is almost free (see the rotational kinetic energy discussed above) and hence $S_{rot} \simeq S_{rot-trans} \simeq 1$.

The effect of changing the LJ parameters on the selectivities for nonspherical H_2 models is reported in Table 5. The S_{trans} values in Table 5 are similar to the selectivities for the effective spherical H_2 model, given in Table 3. This means that even for the modified interactions the minimum value of the potential for a given distance from the tube center corresponds to the molecule almost aligned with the nanotube axis.

The sensitivity of $S_{rot-trans}$ to changes in the LJ diameter and well depth can be observed from the data in Table 5. The contribution of the rotational−translational coupling to the selectivity becomes larger as the steepness of the confining potential increases. As with the translational selectivity, $S_{rot-trans}$ exhibits larger changes for a 10% change in σ_{CC} than for a factor of 2 change in ϵ_{CC}.

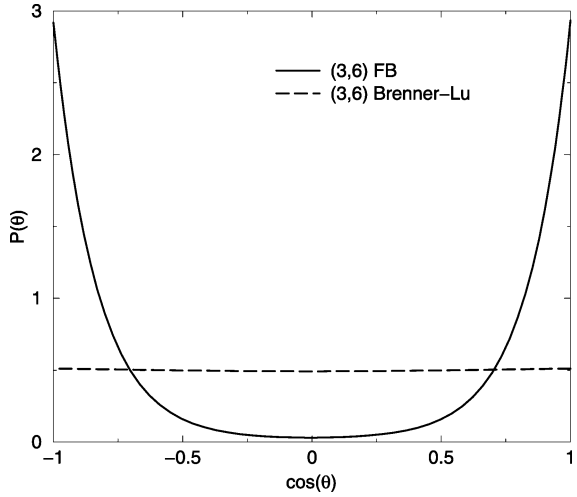

Figure 4. Probability for a H_2 molecule's alignment with respect to the nanotube axis in a (3, 6) SWNT. The solid line is for the FB potential while the dashed line represents the Brenner−Lu potential.

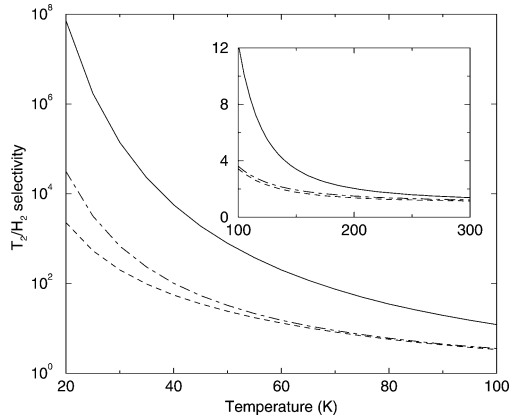

Figure 5. Temperature dependence of the various contributions to the selectivity for the AIREBO potential in the (3, 6) SWNT: solid line, full selectivity; dot−dashed line, translational contribution; dashed line, rotational−translational contribution.

The contribution to the selectivity from the rotational−translational coupling is more sensitive to the values of the interaction parameters than the translational contribution, at least in the case of the (3, 6) tube. If the value of σ_{CC} is raised by 10%, $S_{rot-trans}$ increases by a factor of 250−500 (depending on the model), whereas the translational contribution increases by a factor between 150 and 350. A similar effect is observed if the value of ϵ is modified (see Table 5).

The competing effect between σ and ϵ can be seen by comparing the AIREBO and Steele−Murad potentials. The AIREBO potential has σ_{HC} 3% smaller and ϵ_{HC} 50% larger than the Steele−Murad potential (see Table 2).

The smaller σ parameter would tend to lower the selectivity of AIREBO with respect to Steele−Murad, whereas the higher ϵ would give a trend in the opposite direction. The overall balance between the two competing effects has as a net result that the selectivity of AIREBO is larger −(as reported in Table 4) since the ϵ_{HC} value dominates. When these two potentials are modified, we observe the same situation (see Table 5), except in the case where the σ_{CC} parameter is lowered by 10%.

The approximate treatment of the rotational−translational contribution to the selectivity given in eq 22 is likely to give a lower bound to the actual value. The translational contribution to the selectivity, eq 23, assumes that the molecule is perfectly aligned with the nanotube at any center of mass distance r from the axis. We know from the preceding discussion that this orientation corresponds to the minimum in the potential energy for narrow nanotubes. From a semiclassical point of view, the quantization of the rotational degrees of freedom leads to uncertainty in the orientation at low temperatures, resulting in an effective potential energy that is steeper than for the classical rotor. We have seen in the previous section that a steeper potential results in a higher selectivity. Equation 22, as already pointed out, does not account for the effect of quantized rotation on the translational selectivity.

We briefly comment on the case of heteronuclear molecules. We consider heteronuclear diatomics having the same total mass and same bond length as a corresponding homonuclear diatomic, for example, HT and D_2, where we constrain the bond length for HT to be the same as for D_2. There are three main differences between heteronuclear and similar homonuclear molecules: (1) The center of mass does not correspond to the geometric center of the molecule for heteronuclear molecules. This property means that rotational−translational coupling is especially important, such that eq 3 may be a worse approximation than for a similar homonuclear molecule. However, eq 24 will still be valid. (2) The moment of inertia for heteronuclear molecules is less than that for a similar homonuclear molecule. This means that heteronuclear molecules will have larger rotational constants. (3) The potential energy of a heteronuclear molecule does not fulfill the property $V(r; \theta, \phi) = V(r; \theta, (\pi - \phi))$, giving a different potential energy matrix and excluding the possibility of ortho and para states. Hence, the allowable states for

TABLE 6: Selectivity for T_2/H_2 at 20 K in Various Tubes, Using the FB Potential as In Ref 32

tube type	S_{rot}	$S_{rot-trans}$	S_{trans}	S_0	S_0 (from ref 32)
(3, 6)	2×10^4	4.5×10^4	3.3×10^5	1.51×10^{10}	1.7×10^{10}
(8, 0)	5060	10^4	10^5	10^9	8.2×10^9
(2, 8)	1.15	1.74	31.5	54.8	129
(6, 6)	1.22	0.91	2.61	2.38	3.13
(10, 10)	2.12	0.72	9.47	6.81	15.6

heteronuclear molecules are $J = 0, 1, 2, ...$, whereas $J = 0, 2, 4, ...$ are the allowable states for homonuclear molecules, considering only para-H_2, ortho-D_2, etc.

It is not clear how the three factors identified above will influence the selectivity. We consider here a specific example in order to compare selectivities for heteronuclear and similar homonuclear mixtures. We have calculated the rotational−translational contribution to the selectivity given by eq 24 for T_2/D_2 and QD/TH in the (3, 6) and (2, 8) nanotubes using the Steele−Murad potential, where we denote by "Q", "quartium", an unphysical isotope of hydrogen with three neutrons. These two model mixtures are designed to have the same mass but different symmetry (homonuclear in the first case and heteronuclear in the second). Therefore, any differences in the selectivities are due to differences in the symmetry properties and mass distribution.

Our calculations indicate that the asymmetric mass distribution does indeed have an influence on the selectivity. The rotational−translational coupling calculated using eq 24 is higher for heteronuclear than for similar homonuclear molecules. In particular, both pairs have a translational selectivity $S_{trans} = 19.6$ in the (3, 6) SWNT, but the rotational−translational contribution is $S_{rot-trans} = 31.4$ for QD/TH and $S_{rot-trans} = 14.5$ for T_2/D_2. In the case of the (2, 8) SWNT, $S_{trans} = 2.11$ for both pairs, but QD/TH has $S_{rot-trans} = 1.93$ and T_2/D_2 has $S_{rot-trans} = 1.03$.

III.C. Temperature Dependence of the Selectivity. The temperature dependence of the selectivity of the AIREBO model, calculated with the approximate treatment of the rotational−translational coupling, eq 24, is plotted in Figure 5. The selectivity approaches unity at high temperatures, reaching a value $S_0 = 1.38$ at $T = 300$ K. In the high-temperature (classical) regime, the differences between the two isotopes are vanishingly small. The data in Figure 5 are in qualitative agreement with the temperature dependence of S_0 reported by Lu et al.[24] and by Challa et al.[20]

The contributions to the selectivity from S_{trans} and $S_{rot-trans}$ become nearly equal as the temperature is raised. For example, at 75 K the overall selectivity is around 50, with $S_{trans} = 7.3$ and $S_{rot-trans} = 6.8$. This result points out again the importance of rotational−translational coupling in determining the selectivity. The spherical Brenner−Buch potential gives a selectivity of about 11 at 75 K, almost 5 times lower than the one obtained with a rigid diatomic model for hydrogen. We expect the translational selectivity to be approximately the square root of the fully coupled selectivity at temperatures above about 60 K.

III.D. Selectivities in Larger Tubes. We have used our approximate method to estimate the zero-pressure selectivities in tubes larger than the (3, 6), and we show our results in Table 6, where we also report the results obtained in ref 32 from a direct diagonalization of the full Hamiltonian. Both calculations have been performed with the same potential, namely, the diatomic parametrization of the hydrogen−carbon interaction by FB.[35]

The agreement between our approximate result and the correct value is very good for the narrow (3, 6) tube, where our approximation underestimates the selectivity by about 11%. Our assumption of a molecule almost aligned with the nanotube axis is very well verified in this case.

The agreement is also satisfactory for the (8, 0) and (2, 8) tubes, where our method, despite the inherent approximations, correctly estimates the magnitude of the selectivity. It is clear that as the tube gets wider, the semiclassical approximation of a molecule aligned with the axis is less reliable.

For larger tubes such as the (6, 6) and the (10, 10) we used an approach different than the one outlined in section II.C, because the potential energy profile shows a minimum at a distance $r \neq 0$. In this case, one cannot assume that a molecule is likely to be aligned with the tube axis. To estimate the potential acting on the translational degrees of freedom, we have calculated, for each value of the coordinate r, the minimum of the solid−fluid interaction potential with respect to the molecular orientation, $V_{min}(r) = \min_{\theta,\phi} V(r; \theta, \phi)$. We have then used $V_{min}(r)$ instead of $V_{ll}(r)$in order to perform the calculations outlined in section II.C. This procedure gives the widest possible potential for estimating the molecular densities $\rho(r)$, which in turn gives the lowest possible values for the translational contribution S_{trans} (see eq 22) for these tubes.

This method performs reasonably well. We predict a selectivity that is about a half of the correct result in the (6, 6) and (10, 10) tubes.[32] However, for the (6, 6) and (10, 10) tubes rotational−translational coupling is less than unity, which is an unphysical result.

The values of $S_{rot-trans} < 1$ in the (6, 6) and (10, 10) nanotubes reflect the fact that our approximate method is not accurate for computing the coupling between rotational and translational degrees of freedom for these systems. In particular, we have to assume a particular orientational configuration to calculate $V_{min}(r)$ (or $V_{ll}(r)$ in the case of the narrowest tubes) and neglect the influence of the rotational degrees of freedom on the center of mass density $\rho(r)$ (due to the assumption in eq 11). These effects are important in larger nanotubes, and therefore our method fails. In this case, a more physically reasonable estimate of the actual selectivity can be made by assuming decoupling and using eq 3, with S_{rot} calculated at the position where $V_{min}(r)$ has a minimum. The S_{rot} values are also reported in Table 6. If we assume decoupling for the (6, 6) and the (10, 10) SWNTs, the predicted selectivities are 3.18 and 20.08, respectively, slightly overestimated compared with the exact results.[32]

IV. Conclusions

We have investigated the effects of the solid−fluid potential on the zero-pressure selectivity of para-T_2/para-H_2 in carbon nanotubes, with a particular emphasis on the (3, 6) tube. Six different potential models for H_2-nanotube interactions were studied. Five of the potentials are in qualitative agreement, giving selectivities at 20 K ranging from 2.63×10^4 to 6.05×10^5 when only the translational degrees of freedom are taken into account. The Brenner−Lu potential[24] gives anomalously small selectivities, which can be attributed to the use of an incorrect value for σ_{CC}.

Selectivities are very sensitive to the values of the LJ diameters used in the potentials. A change in σ_{CC} of 10% can give rise to a change in S_0 of about 2 orders of magnitude. The selectivity is less sensitive to the well depth parameter, ϵ_{CC}. A factor of 2 increase in ϵ_{CC} is required to observe a change in the selectivity of about an order of magnitude.

We have analyzed the contribution of the rotational degrees of freedom to the selectivity, using an approximate formula to evaluate the effect of the rotational−translational coupling. Our

approximate model, which is reasonably accurate in the case of narrow tubes, gives a lower bound to the actual value of the rotational−translational coupling to the selectivity, because we do not include the effect of the rotational state on the translational wave function in the calculation of the selectivity. This is evident when our approximate model is applied to larger tubes, where an unphysical value of $S_{\mathrm{rot-trans}} < 1$ is obtained.

The rotational states have a significant effect on the overall selectivity. The rotational−translational coupling approximately gives rise to a multiplicative factor on the order of 10^3-10^4 in the case of the (3, 6) tube. In larger tubes our method is less reliable but nonetheless indicates that the contribution of the rotational degrees of freedom to the overall selectivity is less and less important as the geometrical tube radius grows.

Finally, we comment on the reasons for the discrepancy in previous simulations of quantum sieving, as summarized in Table 1. The very small selectivity predicted by Lu and co-workers[24] is due to the use of an unphysical solid−fluid potential. The selectivity in the (5, 5) SWNT predicted by Gordillo et al.[22] is smaller by a factor of 20 than the selectivity in previously published work.[20] This factor is mainly due to differences in the potentials used. We have calculated the selectivity for T_2/H_2 using the potential parameters reported by Gordillo et al.[22] We calculated $S_0 = 47$ from the product of eq 23 and eq 24, while Gordillo and co-workers report a value of $S_0 = 22.8$.[22] The remaining factor of 2 difference may be due to differences between the diffusion Monte Carlo approach used by Gordillo et al. and the formalism presented here. The factor of 2 difference between T_2/H_2 selectivities in the (10, 10) SWNT reported by Challa et al.[20] and Lu et al.[24] is largely due to the inclusion of rotational states in the latter calculation. Finally, the very large value of D_2/H_2 selectivity inside an interstice reported by Trasca and co-workers[25] cannot solely be accounted for by inclusion of rotational states. The unusual form of the potential used in their calculations is most likely the source of the discrepancy between their result and the result of Challa and co-workers.[21]

Acknowledgment. We thank Donald Brenner, Jeffrey Frey, and Evelyn Goldfield for helpful discussions. We thank one of the reviewers for bringing up the issue of heteronuclear diatomics.

References and Notes

(1) Migone, A. D.; Talapatra, S. Gas Adsorption on Carbon Nanotubes. In *Encyclopedia of Nanoscience and Nanotechnology;* Nalwa, H. S., Ed.; American Scientific: Stevenson Ranch, CA, 2004; Vol. 3.

(2) Bottani, E. J., Tascón, J. M. D., Eds.; *Adsorption by Carbons;* Elsevier: Oxford, 2005.

(3) Vidales, A. M.; Crespi, V. H.; Cole, M. W. *Phys. Rev. B* **1999**, *58*, R13426−R13429.

(4) Teizer, W.; Hallock, R. B.; Dujardin, E.; Ebbesen, T. W. *Phys. Rev. Lett.* **1999**, *82*, 5305−5308.

(5) Teizer, W.; Hallock, R. B.; Dujardin, E.; Ebbesen, T. W. *Phys. Rev. Lett.* **2000**, *84*, 1844−1845.

(6) Talapatra, S.; Zambano, A. Z.; Weber, S. E.; Migone, A. D. *Phys. Rev. Lett.* **2000**, *85*, 138−141.

(7) Stan, G.; Bojan, M. J.; Curtarolo, S.; Gatica, S. M.; Cole, M. W. *Phys. Rev. B* **2000**, *62*, 2173−2180.

(8) Gatica, S. M.; Stan, G.; Calbi, M. M.; Johnson, J. K.; Cole, M. W. *J. Low Temp. Phys.* **2000**, *120*, 337−359.

(9) Kuznetsova, A.; Yates, J. T., Jr.; Liu, J.; Smalley, R. E. *J. Chem. Phys.* **2000**, *112*, 9590−9598.

(10) Simonyan, V. V.; Johnson, J. K.; Kuznetsova, A.; Yates, J. T., Jr. *J. Chem. Phys.* **2001**, *114*, 4180−4185.

(11) Gatica, S. M.; Bojan, M. J.; Stan, G.; Cole, M. W. *J. Chem. Phys.* **2001**, *114*, 3765−3769.

(12) Zambano, A. J.; Talapatra, S.; Migone, A. D. *Phys. Rev. B* **2001**, *64*, 075415.

(13) Talapatra, S.; Migone, A. D. *Phys. Rev. Lett.* **2001**, *87*, 206106.

(14) Muris, M.; Dupont-Pavlovsky, N.; Bienfait, M.; Zeppenfeld, P. *Surf. Sci.* **2001**, *492*, 67−74.

(15) Byl, O.; Kondratyuk, P.; Foth, S.; FitzGerald, S.; Yates, J. T., Jr.; Chen, L.; Johnson, J. K. *J. Am. Chem. Soc.* **2003**, *125*, 5889−5896.

(16) Kahng, Y. H.; Hallock, R. B.; Dujardin, E.; Ebbesen, T. W. *J. Low Temp. Phys.* **2002**, *126*, 223−228.

(17) Wilson, T.; Tyburski, A.; DePies, M. R.; Vilches, O. E.; Becquet, D.; Bienfait, M. *J. Low Temp. Phys.* **2002**, *126*, 403−408.

(18) Calbi, M. M.; Cole, M. W. *Phys. Rev. B* **2002**, *66*, 115413.

(19) Wang, Q.; Challa, S. R.; Sholl, D. S.; Johnson, J. K. *Phys. Rev. Lett.* **1999**, *82*, 956−959.

(20) Challa, S. R.; Sholl, D. S.; Johnson, J. K. *Phys. Rev. B* **2001**, *63*, 245419.

(21) Challa, S. R.; Sholl, D. S.; Johnson, J. K. *J. Chem. Phys.* **2002**, *116*, 814−824.

(22) Gordillo, M. C.; Boronat, J.; Casulleras, J. *Phys. Rev. B* **2001**, *65*, 014503.

(23) Hathorn, B.; Sumpter, B.; Noid, D. *Phys. Rev. A* **2001**, *64*, 022903.

(24) Lu, T.; Goldfield, E. M.; Gray, S. K. *J. Phys. Chem. B* **2003**, *107*, 12989−12995.

(25) Trasca, R. A.; Kostov, M. K.; Cole, M. W. *Phys. Rev. B* **2003**, *67*, 035140.

(26) Tanaka, H.; Kanoh, H.; Yudasaka, M.; Iijima, S.; Kaneko, K. *J. Am. Chem. Soc.* **2005**, *127*, 7511−7516.

(27) Katorski, A.; White, D. *J. Chem. Phys.* **1964**, *40*, 3183−3194.

(28) Moiseyev, N. *J. Chem. Soc., Faraday Trans. 1* **1975**, *71*, 1830−1837.

(29) Beenakker, J. J. M.; Borman, V. D.; Krylov, S. Y. *Chem. Phys. Lett.* **1995**, *232*, 379−382.

(30) Stan, G.; Cole, M. W. *J. Low Temp. Phys.* **1998**, *110*, 539−544.

(31) Kostov, M. K.; Cheng, H.; Herman, R. M.; Cole, M. W.; Lewis, J. C. *J. Chem. Phys.* **2002**, *116*, 1720−1724.

(32) Lu, T.; Goldfield, E. M.; Gray, S. K. *J. Phys. Chem. B* **2005**, *110*, 1742−1751.

(33) Buch, V. *J. Chem. Phys* **1994**, *100*, 7610.

(34) Wang, Q.; Johnson, J. K.; Broughton, J. Q. *Mol. Phys.* **1996**, *89*, 1105−1119.

(35) Frankland, S. J. V.; Brenner, D. W. *Chem. Phys. Lett.* **2001**, *334*, 18−23.

(36) Goldfield, E. M. Private communication, 2004.

(37) Yildirim, T.; Harris, A. B. *Phys. Rev. B* **2003**, *67*, 245413.

(38) Buch, V. *J. Chem. Phys.* **1994**, *100*, 7610−7629.

(39) Steele, W. *J. Phys. Chem.* **1978**, *82*, 817.

(40) Stuart, S. J.; Tutein, A. B.; Harrison, J. A. *J. Chem. Phys.* **2000**, *112*, 6472−6486.

(41) Murad, S.; Gubbins, K. Molecular Dynamics Simulations of Methane Using a Singularity Free Algorithm. In *Computer Modeling of Matter*; American Chemical Society: Washington, DC, 1978; Vol. 86.